Silicon for Spintronic Applications:
Strain-Enhanced Valley Splitting

V. Sverdlov, O. Baumgartner, T. Windbacher, and S. Selberherr
Institute for Microelectronics, TU Wien
Gußhausstraße 27-29/E360, A-1040 Wien, Austria

1. Introduction

The rapid increase in computational power and speed of integrated circuits is supported by the incessant downscaling of semiconductor devices. Thanks to constantly introduced innovative changes in the technological processes, the miniaturization of MOSFETs epitomized by Moore's Law successfully continues. The recently introduced 32 nm technology[1] involves improved high-κ gate stack dielectrics integrated with metal gates. These advances, first introduced for the 45 nm MOSFET process technology by Intel,[2] represent some of the major changes in the technological processing since the invention of MOSFETs. Although alternative channel materials with mobility higher than in silicon have already been investigated,[3,4] it is believed that silicon will remain the main channel material for MOSFETs beyond the 32 nm technology node.

With scaling apparently approaching its fundamental limits, the semiconductor industry is facing critical challenges. New engineering solutions and innovative techniques are required to improve CMOS device performance. Strain-induced mobility enhancement, first introduced for the 90 nm technology node, is now routinely used to increase the device performance. With the 4th generation of stressors employed in the 32nm node,[1] strain technology will certainly maintain its key position among engineering solutions for future technology generations. In addition, new device architectures based on multi-gate structures with better electrostatic channel control and reduced short-channel effects are attracting increased attention. A multi-gate MOSFET architecture is expected to be introduced for the 22 nm technology node. Combined with a high-κ dielectric/ metal gate technology and strain engineering, a multi-gate MOSFET appears to be the ultimate device for high-speed operation with excellent channel control, reduced leakage currents, and low power budget. Confining carriers within a thin film reduces the channel dimension in the transverse direction, which further improves gate channel control.

At the same time the search for post-CMOS device concepts has accelerated. In principle, quantum computation promises to open new horizons to approach large-scale computations. Quantum-mechanical properties used in the data structure architecture are speculated to lead to substantial advantages over classical approaches. Although the concept is very attractive, thus far quantum calculations

have been demonstrated on a small number of qubits only. Several extremely challenging problems prevent the building of a large quantum computer, and more research is needed. One particular problem is how to increase the quantum state coherence within qubits so that the quantum information is not lost before an acceptable number of operations is performed.

Spin as a degree of freedom is promising for future nanoelectronic and spintronic applications. A recently proposed concept of a racetrack memory[5] is based on the controlled domain wall motion by spin-polarized current in magnetic nanowires. Nonvolatile spin-torque based memory elements combined with gate-all-around MOSFETs are a sound option for a future computer architecture with reduced heat generation.[6]

Silicon, the main element of microelectronics, possesses several properties attractive for spintronic applications. Silicon is composed of nuclei with predominantly zero spin, which greatly reduces fluctuations of local magnetic fields and increases the spin coherence time. Silicon is also characterized by a small spin-orbit coupling. In a recent groundbreaking experiment, coherent spin propagation was demonstrated through an undoped silicon wafer of 350 μm thickness.[7] The experiment was made possible by a unique injection and detection technique of polarized spins delivered through thin ferromagnetic films. Coherent propagation of spins over such long distances makes the fabrication of spin-based switching devices likely already in the near future.

Spin-controlled qubits may be thought of as a basis for upcoming logic gates. However, the conduction band of silicon contains six equivalent valleys, which is potentially a source of increased decoherence.[8] Since the valleys in bulk silicon are degenerate, their quantum numbers are directly competing with the spin quantum numbers. Thus, for successful applications one should be able to lift the valley degeneracy by independently modifying their energies in a controllable way, so that the valley separation can be made larger than the spin Zeeman splitting.

Due to size quantization in (001) oriented Si/SiGe heterostructures, the valley degeneracy is partly lifted. The four valleys with light quantization mass are characterized by higher subband energies, while the two valleys with heavy quantization mass yield the unprimed subband ladder. Yet, within the effective mass approximation usually employed to describe the conduction band, the unprimed subband ladder is doubly degenerate. In reality, this degeneracy is removed due to a slightly non-parabolic dispersion of the conduction band. The actual value of the valley, or, to be more precise, the unprimed subband splitting, is a source of controversy, because it seems to vary significantly depending on the experimental setup. For instance, Shubnikov-de-Haas measurements in an electron system of a thin silicon film grown on a SiGe substrate reveal that the valley splitting is on the order of tens of microvolts.[9] At the same time, recent experiments on the conductivity measurements of point contacts created by confining a quasi-two-dimensional electron system in lateral direction with the help of additional gates deposited on the top of the silicon film, demonstrate a splitting between equivalent valleys larger than the spin splitting.[9]

In this chapter, we will try to resolve this inconsistency with an accurate ***k·p***-based model for the conduction band in silicon. We demonstrate that the parabolic band approximation usually employed for subband structure calculations of confined electrons in silicon inversion layers is not sufficient for ultrathin films. The ***k·p*** model includes strain and is shown to be accurate up to energies of 0.5 eV. This model can therefore be used to describe the subband structure in thin silicon films, where the subband quantization energy may reach a hundred meV.

We first describe the subband structure in a thin unstrained silicon film and we demonstrate that the peculiarities of the subband dispersion obtained within the two-band ***k·p*** model result in a linear dependence of the valley splitting on the magnetic field. Furthermore, we show that a large valley splitting is observed in experiments on conduction quantization through a quantum point contact in the [110] direction, but the splitting is suppressed in [100] point contacts. Finally, we demonstrate that the valley splitting is considerably enhanced in films strained in [110] direction.

Our main result can be summarized as follows: a large valley splitting in the confined electron system can be induced by a shear strain component applied to the system. Since strain is routinely used by the semiconductor industry to enhance MOSFET performance, it opens a way to introduce a splitting between the unprimed subbands in a controllable way at little additional cost. By a direct analogy to the magnetic field that controls the spin splitting, shear strain allows one to tune the valley splitting independently and efficiently, thus making silicon attractive to spintronic and "valleytronic"[10] applications.

2.   Accurate model for the conduction band in silicon

To describe the conduction band of silicon close to the minimum located at $k_0 = 0.15(2\pi/a)$ away from the X-point, we follow the classic approach of Refs. 11 and 12. The two conduction bands Δ_1 and Δ_2 are degenerate at the X-point and must be included on an equal footing to describe the dispersion close to the X-point minimum. More distant bands separated by larger gaps are treated with the second order ***k·p*** perturbation theory,[12] which results in the following two-band ***k·p*** Hamiltonian:

$$H = \left(\frac{\hbar^2 k_z^2}{2m_l} + \frac{\hbar^2 (k_x^2 + k_y^2)}{2m_t} \right) I + \left(D\varepsilon_{xy} - \frac{\hbar^2 k_x k_y}{M} \right) \sigma_x + \frac{\hbar^2 k_z k_0}{m_l} \sigma_z , \qquad (1)$$

where σ_x and σ_z are the Pauli matrixes, I is the 2x2 unity matrix, m_t and m_l are the transverse and longitudinal effective masses respectively, ε_{xy} denotes the shear strain component, $M^{-1} \approx m_t^{-1} - m_0^{-1}$, and $D = 14$ eV is the shear strain deformation potential.[9] This is the only form of the Hamiltonian in the vicinity of the X-point allowed by symmetry considerations.[12] The two-band Hamiltonian (1) results in the following dispersion relations:

$$E = \frac{\hbar^2 k_z^2}{2m_l} + \frac{\hbar^2(k_x^2 + k_y^2)}{2m_t} \pm \left(\frac{\hbar^2 k_0^2}{m_l}\right)\sqrt{\left(\frac{k_z}{k_0}\right)^2 + \eta^2}\,, \qquad (2)$$

where the negative sign corresponds to the lowest conduction band, and

$$\eta = \frac{m_l(D\varepsilon_{xy} - \hbar^2 k_x k_y / M)}{\hbar^2 k_0^2}.$$

We point out that the energy E and k_z are counted from the X-point.

The $\boldsymbol{k \cdot p}$ model accurately describes the dispersion relation up to energies of about 0.5 eV.[13] It also reproduces correctly the conduction band dispersion under shear strain.[14] Therefore, the $\boldsymbol{k \cdot p}$ Hamiltonian (1) can be used to describe the subband structure in thin silicon films and inversion layers.

3.   Subband dispersion from the $\boldsymbol{k \cdot p}$ theory

For (001) silicon films, the confinement potential gives an additional contribution $U(z)I$ to the Hamiltonian (1). In the effective mass approximation described by (1) with the coefficient in front of σ_x set to zero, the confining potential $U(z)$ is known to quantize the six equivalent valleys of the conduction band of bulk silicon into the four-fold degenerate primed and the two-fold degenerate unprimed subband ladders. In ultrathin films, the unprimed ladder is predominantly occupied and hence the more important. The term with σ_x in (1) couples the two lowest conduction bands and lifts the two-fold degeneracy of the unprimed subband ladder. The additional unprimed subband splitting, or the valley splitting, can be extracted from the Shubnikov-de-Haas oscillations and is typically in the order of a few tens μeV.[9] However, the valley splitting is significantly enhanced in a laterally confined two-dimensional electron gas (2DEG).[9] The valley splitting is usually addressed by introducing a phenomenological intervalley coupling coefficient at the silicon interface.[15] Here we investigate the valley splitting based on the two-band $\boldsymbol{k \cdot p}$ model (1) without introducing any additional parameters.

We approximate the confining potential of an ultra-thin silicon film by a square well potential with infinite potential walls. This is sufficient for the purpose of analyzing the valley splitting in a quasi-2DEG due to interband coupling. The generalization to include a self-consistent potential is straightforward, though numerically involved.[16] Because of the two-band Hamiltonian, the wavefunction Ψ is a spinor with the two components |0> and |1>. For a wavefunction with a spatial dependence of the form $\exp(ik_z z)$, the coefficients A_0 and A_1 and of the spinor components are related via the Schrödinger equation $H\Psi = E(k_z)\Psi$. For a particular energy E there exist four solutions κ_i ($i = 1, \ldots, 4$) for k_z of the dispersion relation (2), whereas the spatial dependence of a spinor component α is in the form $\sum A_\alpha^i \exp(i\kappa_i z)$. The four coefficients are determined by the boundary conditions that both spinor components are zero at the two film interfaces. This leads to the following equations for $k_{1,2} = \kappa_{1,2}/k_0$:

$$\tan\left(k_1 \frac{k_0 t}{2}\right) = \frac{k_2}{\sqrt{k_2^2 + \eta^2} \pm \eta} \frac{\sqrt{k_1^2 + \eta^2} \pm \eta}{k_1} \tan\left(k_2 \frac{k_0 t}{2}\right). \tag{3}$$

The value of

$$k_2 = \sqrt{k_1^2 + 4 - 4\sqrt{k_1^2 + \eta^2}} \tag{4}$$

becomes imaginary at high η values. Then the trigonometric functions in (3) have to be replaced by the hyperbolic ones. Special care must be taken to choose the correct branch of $(k_1^2 + \eta^2)^{1/2}$ in (4): the sign of $(k_1^2 + \eta^2)^{1/2}$ must be alternated after the argument becomes zero.

For arbitrary parameters, Eq. (3) can only be solved numerically. We present results of the numerical solution in the next section. However, to gain an insight into the results it is sufficient to analyze the solutions for small strain.

Introducing $y_n = (k_1 - k_2)/2$, Eq. (3) can be written in the form:[17]

$$\sin(y_n k_0 t) = \pm \frac{\eta y_n \sin\left(\sqrt{\frac{1 - \eta^2 - y_n^2}{1 - y_n^2}} k_0 t\right)}{\sqrt{(1 - y_n^2)(1 - \eta^2 - y_n^2)}} . \tag{5}$$

Applying a perturbation approach to Eq. (5) with η as the small parameter, we obtain the following dispersion relation for the unprimed subbands n:

$$E_n^{\pm} = \frac{\hbar^2}{2m_l}\left(\frac{\pi n}{t}\right)^2 + \hbar^2 \frac{k_x^2 + k_y^2}{2m_t} \pm \left(\frac{\pi n}{k_0 t}\right)^2 \frac{\left|D\varepsilon_{xy} - \dfrac{\hbar^2 k_x k_y}{M}\right|}{k_0 t \left|1 - \left(\pi n / k_0 t\right)^2\right|} \sin(k_0 t) . \tag{6}$$

Equation (6) demonstrates that the unprimed subbands are not necessarily degenerate and degeneracy is preserved only when the shear strain is zero and either $k_x = 0$ or $k_y = 0$.

4.   Splitting of unprimed subbands in magnetic field

For zero shear strain the Landau levels in an orthogonal magnetic field B are found from Eq. (6) by using the Bohr-Sommerfeld quantization conditions:

$$E_m^{(1,2)} = \hbar\omega_C\left(m + \frac{1}{2}\right) \frac{\pi}{4\arctan\left(\sqrt{m_{(1,2)} / m_{(2,1)}}\right)}, \tag{7}$$

where

$$m_{(1,2)} = \left(\frac{1}{m_t} \pm \frac{1}{M} \left(\frac{\pi n}{k_0 t} \right)^2 \frac{\sin(k_0 t)}{k_0 t \, | 1 - \left(\pi n / k_0 t \right)^2 |} \right)^{-1} , \qquad (8)$$

and $\omega_C = eB/(m_1 m_2)^{1/2} c$ is the cyclotron frequency, e is the electron charge, and c is the speed of light. According to (7), the difference $|E_m^{(1)} - E_m^{(2)}|$ varies linearly with the magnetic field.

In Shubnikov-de-Haas experiments there will now occur two sets of resistance oscillations with slightly different periods. Because of the small difference between the masses, the difference in periods will also be small. However, at the Fermi level, the quantum number m, which is proportional to the ratio of the Fermi energy to the cyclotron frequency, is typically very large and may lead to a splitting of several hundred μeV. The difference in the periods can be interpreted as an appearance of an additional energy shift between the equivalent unprimed valleys. Most importantly, the shift is linear in the magnetic field. The linear dependence of the intervalley splitting on the magnetic field will be also observed in the presence of a small intrinsic constant valley splitting, as long as this splitting is much smaller than the Fermi energy. This splitting is possible due to a remaining shear strain and/or conduction band nonparabolicity, which is not accounted for in the two-band $k \cdot p$ theory and which is usually several tens of μeV, thus much smaller than the Fermi energy. For a 10 nm thick silicon film grown on SiGe it follows from (7) and (8) that the valley splitting can be several tens of μeV in a magnetic field of 1 T, which is consistent with the experimental observations.[9]

5.   Splitting between the unprimed subbands in a point contact

Now let us consider a point contact in [110] direction realized by confining an electron system of a thin silicon film laterally by depleting the area under additional gates. Without strain, the low-energy effective Hamiltonian in the point contact can be written as:

$$H_{(1,2)} = \frac{\hbar^2 k_x'^2}{2m_{(2,1)}} + \frac{\hbar^2 k_y'^2}{2m_{(1,2)}} + \frac{1}{2} \kappa x'^2 + V_B \quad , \qquad (9)$$

where the primed variables are along the [1, 1, 0] and [1, −1, 0] axes, the effective masses are determined by (8), κ is the spring constant of the point contact confinement potential $V(x') = \kappa x'^2/2$ in [1, −1, 0] direction, and V_B is a gate voltage dependent conduction band shift in the point contact.[18] The dispersion relation of propagating modes within the point contact can be written as:

$$E_p^{(1,2)} = \frac{\hbar^2 k_x'^2}{2m_{(2,1)}} + \hbar \omega_{(1,2)} (p + \frac{1}{2}) + V_B \quad , \qquad (10)$$

where $\omega_{1,2}^2 = \kappa/m_{1,2}$. Since the energy minima of any two propagating modes with the same p are separated, they are resolved in a conductance measurement through

the point contact as two distinct steps. The valley splitting is $\Delta E_p = \hbar|\omega_1 - \omega_2|$. The difference in the effective masses (8) and, correspondingly, the valley splitting can be significantly enhanced by reducing the effective thickness t of the quasi-2DEG, which is usually the case in a gated electron system, when the inversion layer is formed.

In a [100] oriented point contact without strain, the effective Hamiltonian is

$$H^{\pm} = \hbar^2 \frac{k_x^2 + k_y^2}{2m_t} \pm \left(\frac{\pi n}{k_0 t}\right)^2 \frac{\left|\dfrac{\hbar^2 k_x k_y}{M}\right| \sin(k_0 t)}{k_0 t \,|\, 1 - \left(\pi n / k_0 t\right)^2 \,|} + \frac{\kappa}{2} x^2 .$$

Due to the symmetry with respect to k_y the subband minima in a point contact are always degenerate. For this reason the valley splitting in [100] oriented point contacts is considerably reduced.

6. Strain-enhanced valley splitting

It follows from (6) that shear strain induces a valley splitting linear in strain for small shear strain values:[17]

$$\Delta E_n = 2\left(\frac{\pi n}{k_0 t}\right)^2 \frac{D\varepsilon_{xy}}{k_0 t \,|\, 1 - \left(\pi n / k_0 t\right)^2 \,|} \sin(k_0 t) .$$

The subband splitting is inversely proportional to the film thickness to the third power, and thus can be quite large in thin films.

One can also evaluate the maximum subband splitting in the $\eta \to \infty$ limit. Here, it follows from (2) that the band dispersion becomes parabolic again around the minimum located exactly at the X-point. The subband quantization energies are determined by the usual quantization conditions, which results in the subband splitting

$$\Delta E_n = \left(\frac{\hbar\pi}{t}\right)^2 \frac{2n-1}{2m_t} .$$

For practically relevant intermediate strain values a numerical solution of Eq. (3) is required.

7. Numerical results

In order to analyze the subband structure in (001) oriented thin silicon films we first approximate the film potential by the square well potential with infinite potential walls. Although not exact, this is a good approximation for thin films. To obtain the values for the subband splitting and effective masses for an arbitrary strain value, Eq. (3) can be solved numerically. Alternatively, the eigenvalues can

be found by solving the equations obtained by discretizing the Hamiltonian (1) with the added confinement potential $IU(z)$ and replacing k_z by $-i\partial/\partial z$. The latter method is more general, because it allows the inclusion of a confinement potential of arbitrary form, making self-consistent calculations possible.

We implemented both numerical routines and obtained equivalent results for a square well potential with infinite walls.

The splitting between the unprimed subbands with the same quantum number n normalized to the ground subband energy in unstrained films for a film of thickness $t = 3.2$ nm is shown in Fig. 1 as function of shear strain. The dependence is not monotonic and strongly depends on the subband number. Even for the ground subbands with $n = 1$, the splitting is comparable to the subband energy at large strain values. The subband splitting increases rapidly as the film thickness is decreased, as demonstrated in Fig. 2. For ultrathin body films the splitting can reach a value comparable to $k_{B}T$ already at moderate strain values.

Results shown in Fig. 2 demonstrate that the valley splitting can be effectively controlled by adjusting the shear strain and modifying the effective thickness t of the electron system. Uniaxial stress along [110] channel direction, which induces shear strain, is already used by industry to enhance MOSFET performance. Therefore, its application to control valley splitting does not require expensive technological modifications.
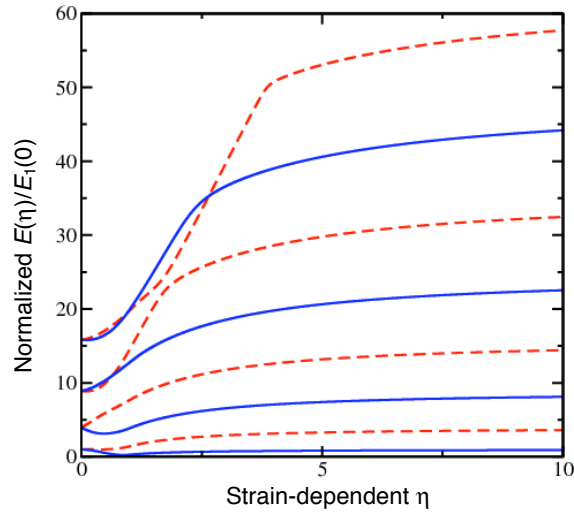

Figure 1. Calculated energies of unprimed subbands in a 3.2 nm thick silicon film as a function of shear strain. The subband energies values are normalized to the energy of the ground subband in an unstrained film. In the unstrained film, the subbands are two-fold degenerate. Strain induces the splitting between the subbands with the same quantum number (shown by solid and dashed lines). The value of the splitting may change sign. The value $\eta = 1$ corresponds to the shear strain value $\varepsilon = 0.016$.
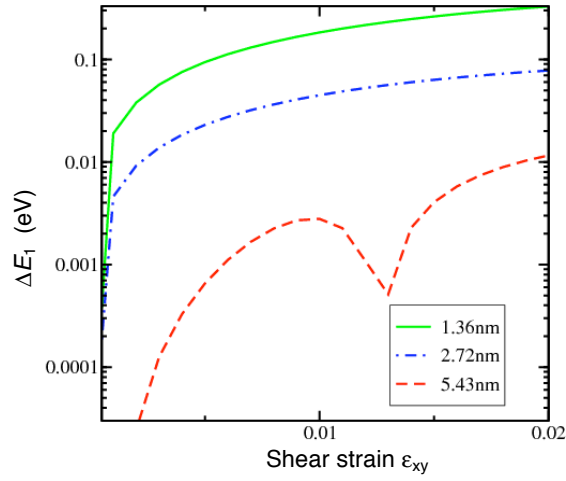
Figure 2. Shear strain-induced splitting of the ground subbands for several film thicknesses. In ultrathin films the splitting exceeds $k_B T$ already for moderate stress.

8. Conclusions

We have analyzed the structure of the unprimed subbands in (001) silicon thin films by using an appropriate **k·p** model and demonstrated that the two-fold degeneracy of the unprimed subbands can be lifted, leading to the so-called valley splitting. In an external magnetic field, the model predicts the value of splitting to be proportional to the field. Furthermore, the model predicts that the valley splitting in a <110>-oriented point contact can be larger than the splitting due to the magnetic field because of stronger lateral confinement in a point contact. Finally, the valley splitting can be successfully controlled by shear strain. This makes silicon promising for spintronic and "valleytronic" applications.

References

1. S. Natarajan, M. Armstrong, M. Bost, *et al.*, "A 32 nm logic technology featuring 2nd-generation high-κ + metal-gate transistors, enhanced channel strain and 0.171 μm^2 SRAM cell size in a 291 Mb array," *Tech. Digest IEDM* (2008), pp. 941–943.

2. K. Mistry, C. Allen, C. Auth, *et al.*, "A 45 nm logic technology with high-κ + metal gate transistors, strained Si, 9 Cu interconnect layers, 193 nm dry patterning, and 100% Pb-free packaging," *Tech. Digest IEDM* (2007), pp. 247–250.

3. M. K Hudait, G. Dewey, S. Datta, *et al.*, "Heterogeneous integration of enhancement mode In$_{0.7}$Ga$_{0.3}$As quantum well transistor on silicon substrate using thin composite buffer architecture for high-speed and low-voltage (0.5V) logic applications," *Tech. Digest IEDM* (2007), pp. 625–628.

4. R. Chau, "Challenges and opportunities of emerging nanotechnology for future VLSI nanoelectronics," *Proc. ISDRS* (2007), p. 3.

5. S. S. P. Parkin, M. Hayashi, and L. Thomas, "Magnetic domain-wall racetrack memory," *Science* **320**, 190 (2008).

6. T. Endoh and T. Hanyu, "Impact of spintronic devices for future nano silicon based LSI," in *Abstracts 5th Intern. School Conf. Spintronics Quantum Inform. Technol. (SPINTECH-V)* (Krakow, 2009), p. 95.

7. I. Appelbaum, B. Huang, and D. J. Monsma, "Electronic measurement and control of spin transport in silicon," *Nature* **447**, 295 (2007).

8. P. Zhang and M. W. Wu, "Spin diffusion in Si/SiGe quantum wells: Spin relaxation in the absence of Dyakonov-Perel' relaxation mechanism," *Phys. Rev. B* **79**, 075303 (2009).

9. S. Goswami, K.A. Slinker, M. Friesen*, et al.*, "Controllable valley splitting in silicon quantum devices," *Nature Phys.* **3**, 41 (2007).

10. A. Rycerz, J. Tworzydlo, and C. W. J. Beenakker, "Valley filter and valley valve in graphene," *Nature Phys.* **3**, 172 (2007).

11. J. C. Hensel, H. Hasegawa, and M. Nakayama, "Cyclotron resonance in uniaxially stressed silicon," *Phys. Rev.* **138**, A225 (1965).

12. G. L. Bir and G. E. Pikus, *Symmetry and Strain-Induced Effects in Semi-conductors*, New York: Wiley, 1974.

13. V. Sverdlov, O. Baumgartner, T. Windbacher, *et al.*, "Impact of confinement of semiconductor and band engineering on future device performance," *Proc. 215th ECS Meeting, Silicon-on-Insulator Technol. Dev.* (2009), pp. 15–26.

14. V. Sverdlov, G. Karlowatz, S. Dhar, *et al.*, "Two-band $k \cdot p$ model for the conduction band in silicon: Impact of strain and confinement on band structure and mobility," *Solid State Electronics* **52**, 1563 (2008).

15. M. Friessen, S. Chutia, C. Tahan, *et al.*, "Valley splitting theory of SiGe/Si/SiGe quantum wells," *Phys. Rev. B* **75**, 115318 (2007).

16. O. Baumgartner, M. Karner, V. Sverdlov, *et al.*, "Numerical quadrature of the subband distribution functions in strained silicon UTB devices," *Proc. 13th Intern. Workshop Comput. Electronics* (2009), pp. 53–56.
17. V. Sverdlov and S. Selberherr, "Electron subband structure and controlled valley splitting in silicon thin-body SOI FETs: Two-band *k·p* theory and beyond," *Solid State Electronics* **52**, 1861 (2008).
18. B. van Wees, H. van Houten, and C. Beenakker, "Quantized conductance of point contacts in a two-dimensional electron gas," *Phys. Rev. Lett.* **60**, 848 (1988).